Statics and dynamics of single polymers confined between two corrugated walls

Debashish Mukherji

Max-Planck Institut für Polymerforschung, Ackermannweg 10, 55128 Mainz, Germany

E-mail: mukherji@mpip-mainz.mpg.de

Martin H. Müser

Jülich Supercomputer Center, Institute for Advanced Simulation, FZ Jülich, 52425 Jülich, Germany

Abstract. Using molecular dynamics, we study static and dynamic properties of isolated linear polymers in good solvent conditions, which are confined between two parallel, corrugated walls. If the distance between the confining walls is so small that the polymer collapses into a single layer, the diffusion constant D is found to scale linearly with the degree of polymerization N. The proportionality constant is sensitive to wall-wall and wall-polymer commensurability. Static properties, such as out-of-plane monomer density profile $n(z)$ and radius of gyration $R_{\rm g}$, obey the scaling laws predicted by Flory's mean field theory.

1. Introduction

Understanding the diffusion of polymers that are confined or constrained by solid walls is not only theoretically challenging [1, 2] but also relevant in various technological applications such as in tribology [3, 4], narrow-channel macromolecular devices [5, 6], and for the possibility to separate macromolecules of different size via confinement [7]. In this context two cases are widely studied: (a) adsorbed linear polymers [8, 9, 10, 11, 12, 13, 14, 15] and (b) polymers confined between two surfaces [16, 17, 18, 19, 20] Experimental advances in this field are made possible due to the application of fluorescence spectroscopy, which allows one to measure, for instance, the mobility of DNA [9, 18, 19, 20] and that of phospholipids [12] on lipid bilayers with the prospect of their use in nano-technology.

Static and dynamic properties of polymers are commonly rationalized in terms of scaling laws [21]. In this paper, we will present molecular dynamics simulations of polymers confined between two parallel, corrugated walls, and examine the effect of wall friction on the center of mass diffusion of the polymers in terms of scaling laws. To produce the correct polymer configurations, we will include the solvent implicitly in the (thermodynamic) interactions between different monomers, but neglect any (implicit) hydrodynamic interaction mediated by the solvent. The latter has to be done in order for us to single out the wall-induced damping. As our simulations will be carried out in equilibrium, and as we are interested in a linear response quantity, namely diffusion, the two damping mechanism can be considered to be additive.

For our study, we will employ the same generic model as in our previous works [13, 14, 15] on polymer diffusion on a single surface. These studies reproduced successfully a variety of

Table 1. Different cases studied in this work. A relative orientation of 90° renders two hexagonal surfaces incommensurate. d is nearest-neighbor distance between surface atoms. $\bar{b}$ represents the intrinsic bond length for a bead spring polymer.

cases	wall orientation	d	b
case 1	incommensurate	1.201	0.97
case 2	commensurate	1.201	0.97
case 3	incommensurate	0.970	0.97
case 4	commensurate	0.970	0.97

experimental observations, among others: (a) The $D \propto N^{-1.5}$ relationship for polymers on a solid surface [10], (b) the $D \propto N^{-1}$ relationship for polymers on an on-overage flat liquid surface [9] and/or lattice models, and (c) the non-monotonic change of mobility of polymers with concentration [11]. An important aspect in our previous work, in particular that on the diffusion of single polymers, turned out to be the commensurability between polymer and surface. This is why bond lengths commensurate and incommensurate with the lattice constant will be considered here too. In addition, the commensurability between the walls may play a role, as even an ideal gas can pin two commensurate walls that do not interact directly with one another [4]. Therefore, we will investigate both, commensurate and incommensurate confining walls.

2. Model and Method

As usual, we assume that chemical detail does not affect the values of critical exponents. This is why we will base our study on a simple, albeit widely used particle-based continuous-space representation of a polymer molecule developed by Kremer and Grest [22] also known as bead-spring model. A more detailed model related discussion is provided in Ref. [13, 14, 15]. In this model, good solvent conditions can be mimicked by having each two monomers interact via a truncated and shifted (purely repulsive) Lennard-Jones (LJ) potential. Adjacent monomers also interact with an additional finitely extensible nonlinear elastic (FENE) potential. The parameters of the potential (i.e., LJ + FENE) is chosen such that no unphysical bond crossing is allowed [22]. In the following, we will express all physical quantities in units of Lennard-Jones (LJ) energy ε, LJ length σ, and mass m of individual monomers. This model gives rise an effective bond length of 0.97 [22].

Temperature is controlled using a Langevin thermostat, which is only applied to the z-component of the monomer's motion, i.e., normal to the interface. Unless stated otherwise, the thermal energy is set to 0.5. The damping coefficient is set to 0.1 in reduced units.

The bead-spring chain is confined between two surfaces, each of which consists of a discrete hexagonal plane, e.g., a (111) plane of a face-centered-cubic solid. Wall atoms are pinned to their hexagonal lattice sites. The geometry of the surface is square with fixed linear dimensions 75.0. In the case of the nearest neighbor distance 0.97, we increased the number of unit cells in the lateral dimension to attain same linear dimensions 75.0. Periodic boundary conditions are applied only along the lateral directions, i.e., in the (x, y)-plane. In each MD run, the separation δ between the two walls is kept fixed. The orientations of the two surfaces are usually parallel, however, upon extreme confinement, i.e., for $\delta \leq 7.5$, we also investigate effectively incommensurate interfaces. These are produced by rotating one of the two hexagonal walls by 90°. We studied four cases as listed in table 1.

The interaction between a wall atom and a monomer is the same LJ potential as the one acting between two monomers. When investigating the dependence of an observable as a function of δ,

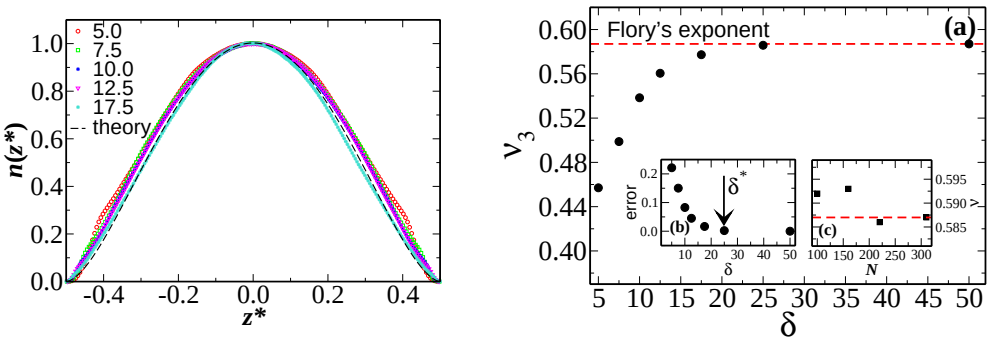

Figure 1. (Left panel) Out-of-plane monomer density profile, $n(z^*)$, for different inter-wall distances, δ. Here $z^* = \tilde{z}/\tilde{\delta}$ with $\tilde{\delta} = \delta - 1.5$ and $\tilde{z} = z - 1.5/2$. The dashed curve is a fit based on Eq. 1 using the exact value $\nu_3 = 0.587$ [21]. (Right panel) (a) The (apparent) exponent ν as obtained for different inter-wall distances δ at $N = 220$. ν_3 is calculated by fitting $n(z)$ to the power-law z^{1/ν_3} at small values of z/δ. (b) Absolute, relative difference between apparent and exact exponent ν_3, $(0.587 - \nu_3)/0.587$, as a function of δ. The arrow indicates the value for δ that satisfies equation (2). (c) (Apparent) exponent ν_3 for different chain lengths calculated for $\delta = \delta^*$. The exact exponent is represented by the horizontal dashed line.

we restrict the degree of polymerization to the two values $N = 160$ and $N = 220$. The distance between the walls is varied from $\delta = 2.5$ to $\delta = 26.5$. When keeping δ fixed to study chain length effects, we vary N within $40 \leq N \leq 310$.

The equations of motion are integrated using a fifth order predictor-corrector method with time step $\Delta t = 0.005$. Simulations are usually equilibrated for a few hundred million MD time steps and then observation is carried out over another $50 \cdot 10^6$ MD time steps, i.e., over a time span $2.5 \cdot 10^5$ (in LJ units). During this observation period, quantities of interest such as the the radius of gyration R_g, diffusion coefficient D and out-of-plane monomer density profile $n(z)$ are measured.

3. Model validation

We would like to start by demonstrating that the used model produces the proper polymer configurations and also that the employed degree of polymerization suffices to be within the proper scaling regime. For this purpose, we will investigate the density profile as well as the in-plane and out-of-plane radius of gyration, which depend on δ via well-established power laws [21].

3.0.1. Monomer density profile

The monomer density $n(\Delta z)$ of a single polymer near a flat, impenetrable wall has been predicted by Flory in a mean-field theory to follow a $n(\Delta z) \propto \Delta z^{\nu_3}$ power law, where ν_d is given as, $\nu_d = 3/(d+2)$, so that $\nu_3 = 0.6$. Here Δz denotes the distance of a monomer from the wall. The value for the exact exponent, namely $\nu_3 = 0.587$ [21], is fairly close to the mean-field value.

When two walls are present the following dependence of the density on the z-coordinate is observed [21]:

$$n(z^*) \propto \left(\frac{1}{4} - z^{*2}\right)^{1/\nu_3}, \tag{1}$$

Table 2. Apparent exponent ν_3 for different wall separations and chain lengths. Included is information on the radius of gyration in the bulk solution, $R_{\mathbf{gb}}$.

N	$R_{\rm gb}$	δ^*	ν_3
100	7.5 ± 0.3	16.5	0.591
160	9.6 ± 0.4	21.5	0.593
220	11.6 ± 0.7	25.0	0.586
310	14.2 ± 0.8	30.0	0.587
Theory			0.587

where we have normalized the value for z with δ and also subtracted a correction due to the finite size of wall atoms, specifically $z^* = \tilde{z}/\tilde{\delta}$ with $\tilde{\delta} = \delta - 1.5$ and $\tilde{z} = z - 1.5/2$. The rationale for this correction is the following one: The atoms of the bottom solid sit at $z = 0$ while those at the top solid sit at $z = \delta$. Monomers can approach these positions only up to a distance that is close to the wall-atom monomer Lennard-Jones interaction distance. Thus the lowest value of $\tilde{z}$ where monomers can sit is close to zero and the largest value is close unity. Precise values cannot be stated, because walls are slightly corrugated and also because the walls are not ideally hard. In the left panel of Fig. 1, we show the normalized data for $n(z)$. It can be appreciated that the data for different cases collapse onto one master plot which is consistent with Eq. (1).

It is well known, that the exponent ν_3 can only be obtained at sufficiently large inter-wall separation [17, 21]. In our simulations, we observe that the exact exponent can be reproduced within 1% if the following inequality is obeyed:

$$\delta \geq \delta^* = 2R_{\rm gb} + 1.5\sigma_{\rm sp}, \tag{2}$$

where $R_{\rm gb}$ is the bulk radius of gyration. To validate the claim that the choice $\delta \geq \delta^*$ will lead to a very good approximation to the exact value of ν_3, we included part (a) in Fig. 1, whose main part shows how the apparent exponent ν_3 changes with δ at fixed $N = 220$. The more detailed analysis in inset (b) shows that the deviation between our data and the predicted exponent decreases with δ, while inset (c) demonstrates that Flory's exact exponent can be observed within 1% accuracy for different chain lengths N as long as our rule, Eq. (2), is obeyed.

The data leading to part (c) of Fig. 1 is shown in table 2. Included are also the values we obtained for the bulk radius of gyration $R_{\rm gb}$, which was calculated from single polymers in the absence of any confining walls.

3.0.2. Chain conformation We now direct our focus on the chain conformation. The quantity that best describes the polymer conformation in simple terms is the tensor of gyration $T_{\alpha\beta}(\delta)$,

$$T_{\alpha\beta}(\delta) = \frac{1}{N}\left\langle \sum_{i=1}^{N} (R_{i\alpha} - \bar{R}_\alpha)(R_{i\beta} - \bar{R}_\beta) \right\rangle, \tag{3}$$

where α and β indicate the Cartesian indices. $R_{i\alpha}$ is the α^{th} component of the i^{th} monomer position, and $\bar{R}_\alpha$ is the α^{th} component of the center-of-mass of the chain. In the following, we will distinguish between the in-plane radius of gyration, $R^2_{\rm g||} = T_{xx} + T_{yy}$, and the out-of-plane radius of gyration, $R^2_{\rm g\perp} = T_{zz}$.

The following scaling laws are established [17, 21] for in-plane and out-of-plane radius of gyration in the limit of small δ:

$$R^2_{\rm g||}(\delta) \propto \delta^{-2(\nu_2-\nu_3)/\nu_3}, \tag{4}$$

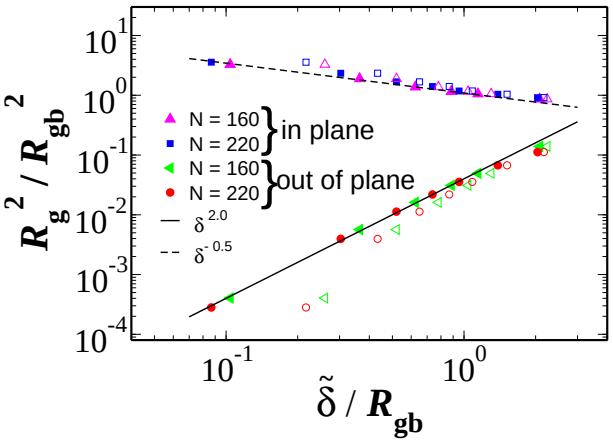

Figure 2. (color online) Normalized radius of gyration squared as a function of normalized inter-wall distance for two different chain lengths. Where $\tilde{\delta} = \delta - 1.5$ in the case of solid symbols and open symbols correspond to $\tilde{\delta} = \delta$. Lines are power law fits according to Eqs. (4-5) and mean-field values for Flory's exponents.

and

$$R^2_{g\perp}(\delta) \propto \delta^2, \tag{5}$$

where ν_d is Flory's exponent in d dimensions and defined as $3/(d+2)$.

In the analysis of our simulation data, we will compare the numerical data to the mean field value of ν_d rather than to the exact exponent ν [21], because our error bars are not sufficiently small to discriminate between the two. Results are depicted in Fig. 2 for two different chain lengths. By normalizing the value of δ, $R_{g||}$, and $R_{g\perp}$ with R_{gb}, results for the two different chain length could be collapsed. In addition, by subtracting the excluded-volume "offset" of $1.5\sigma_{sp}$ from δ, the power-law dependence $R^2_{g||} \propto \tilde{\delta}^{-1/2}$ and $R^2_{g\perp} \propto \tilde{\delta}^2$ could be borne out on a larger domain at small wall separations. Of course, at large values of $\tilde{\delta}$, the scaling laws valid for small $\tilde{\delta}$ must break down, because for $\tilde{\delta} \geq R_{gb}$, the configurations become bulk-like, and thus $R^2_{g||}$ approaches $2R^2_{gb}/3$ and $R^2_{g\perp}$ approaches $R^2_{gb}/3$.

4. Results for polymer dynamics

Having reproduced the known static behavior of a confined polymer chain, we now direct our focus on dynamic properties. We investigate how D changes with N at fixed separation between two walls. Results for $\delta = 2.5$ are summarized in Fig. 3, in one case we also reduce $\delta = 2.0$. For polymer bond lengths commensurate with the walls, we had to increase the temperature from $T = 0.5$ to $T = 0.6$, in order to speed up polymer diffusion for accurate measurements. The data can be fit via Rouse dynamics, namely $D \propto N^{-1}$, in all cases for $\delta = 2.5$. Looking into the simulation snapshot we find that polymers essentially form a flat monolayer configuration. Therefore, this flat polymer is "rubbing" against the repulsive walls so that the damping (i.e., the inverse diffusion constant) of the polymers centroid is simply proportional to the number of monomers in contact with the surfaces. This argument explains why we observe a scaling linear in N.

It may be worth comparing these results to those found when a single polymer is strongly adsorbed onto only one wall, which however is so strongly adhesive that the polymer collapses into a single layer. For the strongly adhesive single wall, commensurability plays a role, while in the new study it does not. Specifically, for a single adhesive wall, we had found $D \propto N^{-1}$ for a polymer whose bond lengths are commensurate with the substrate and $D \propto N^{-1.5}$ for the incommensurate case. Thus, our new simulations show similarity with the commensurate, single-wall case and so there appears to be a contradiction: If two walls are commensurate with each other but incommensurate with the polymer, then in the limit of a single-layer confinement, one should produce the $N^{-1.5}$ and not the $1/N$ scaling of D. This issue can be resolved as follows: In our previous work we had shown that the $N^{-1.5}$ is only born out if N is sufficiently

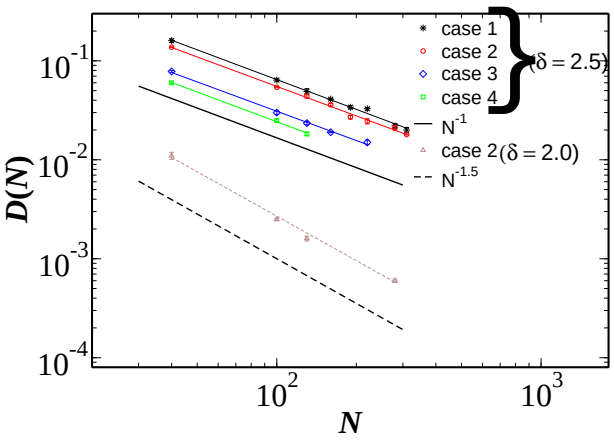

Figure 3. (color online) In-plane chain lateral diffusion D as a function of chain length N. Results are shown for both commensurate and incommensurate surfaces as mentioned in table 1 for $\delta = 2.5$. For cases 3 and 4 we increase the temperature from $T = 0.5$ to $T = 0.6$. Line are fits with the exponent shown in caption.

large and/or the walls sufficiently rough. Small roughness first produced N^{-1} scaling at small N before crossing over the $N^{-3/2}$ dependence. The small-roughness regime is what we see in the present study at $\delta = 2.5$. If we reduce the separation between the two walls to $\delta = 2$, we recuperate the $N^{-3/2}$ scaling law for an incommensurate polymer between incommensurate surface, because at this small separation, corrugation becomes large.

5. Conclusions

We use molecular dynamics simulations to study the static and dynamics of confined polymer chain. Static properties, such as radius of gyration and out-of-plane monomer density profile, follow the predicted scaling behavior. Chain length dependent lateral dynamics follow Rouse behavior, unless the confinement is extreme, in which case $D \approx N^{-3/2}$ for incommensurate polymer-wall geometries.

References

[1] S. S. Patel and M. Tirrel, Annu. Rev. Phys. Chem. **40**, 597 (1989).
[2] E. Eisenriegler, *Polymers near surfaces* (World Scientific, Singapore, 1993).
[3] S. Granick et. al., J. Pol. Sci. B, **41**, 2755 (2003).
[4] M. H. Müser and M. O. Robbins, Phys. Rev. B **61**, 2335 (2000).
[5] O. B. Bakajin, T. A. J. Duke, C. F. Chou, S. S. Chan, R. H. Austin, and E. C. Cox, Phys. Rev. Lett. **80**, 2737, (1998).
[6] W. Reisner, K. J. Morton, R. Riehn, Y. M. Wang, Z. Yu, M. Rosen, J. C. Sturm, S. Y. Chou, E. Frey, and R. H. Austin, Phys. Rev. Lett. **94**, 196101, (2005).
[7] J. Han and H. Craighead, Science **288**, 1026 (2000).
[8] A. Milchev and K. Binder, Macromolecules **29**, 343 (1996).
[9] B. Maier and J. O. Rädler, Phys. Rev. Lett. **82**, 1911 (1999).
[10] S. A. Sukhishvili, Y. Chen, J. D. Müller, K. S. Schweizer, E. Gratton, and S. Granick, Nature **406**, 146 (2000).
[11] J. Zhao and S. Granick J. Am. Chem. Soc. **126**, 6242 (2004).
[12] L. Zhang and S. Granick, Proc. Nat. Acad. Sci. U.S.A. **102**, 9118 (2005).
[13] D. Mukherji and M. H. Müser, Phys. Rev. E. **74**, 010601(R) (2006).
[14] D. Mukherji and M. H. Müser, Macromolecules **40**, 1754 (2007).
[15] D. Mukherji, G. Bartels and M. H. Müser, Phy. Rev. Lett. **100**, 068301 (2008).
[16] F. Brochard and P.-G. de Gennes, J. Chem. Phys. **67**, 52 (1977).
[17] A. Milchev and K. Binder, Eur. Phys. Jour. B **3**, 477 (1998).
[18] Y. L. Chen, M. D. Graham, J. J. de Pablo, G. C. Randall, M. Gupta and P. S. Doyle, Phys. Rev. E. **70**, 60901 (2004).
[19] A. Balducci, P. Mao and P. S. Doyle, Macromolecules **39**, 6273 (2006).
[20] A. Balducci, J. Tang, and P. S. Doyle, Macromolecules **41**, 9914 (2008).
[21] P.-G. de Gennes, *Scaling Concepts in Polymer Physics* (Cornell University Press, London, 1979).
[22] K. Kremer and G. S. Grest, J. Chem. Phys. **92**, 5057 (1990).